NJC

PAPER

View Article Online
View Journal



Cite this: DOI: 10.1039/c8nj02979b

# Preparation of hydrido [CNC]-pincer cobalt complexes *via* selective C–H/C–F bond activation and their catalytic performances†

Fei Yang,[a] Yangyang Wang,[ab] Faguan Lu,[a] Shangqing Xie,[a] Xinghao Qi,[a] Hongjian Sun,[a] Xiaoyan Li,*[a] Olaf Fuhr[c] and Dieter Fenske[c]

Polyfluorinated aryl imines 2,4,5-$R_1$,$R_2$,$R_3$-$C_6H_2$-HC═N-1-$C_{10}H_7$ ($R_1$ = F, $R_2$ = F, $R_3$ = H (**1**); $R_1$ = F, $R_2$ = H, $R_3$ = F (**2**) and $R_1$ = F, $R_2$ = F, $R_3$ = F (**3**)) and $F_5C_6$-HC═N-1-$C_{10}H_7$ (**7**) reacted with $CoMe(PMe_3)_4$ to give rise to hydrido [CNC]-pincer cobalt(III) complexes (2,4,5-$R_1$,$R_2$,$R_3$-$C_6$H-HC═N-1-$C_{10}H_6$)Co(H)$(PMe_3)_2$ ($R_1$ = F, $R_2$ = F, $R_3$ = H (**4**); $R_1$ = F, $R_2$ = H, $R_3$ = F (**5**); $R_1$ = F, $R_2$ = F, $R_3$ = F (**6**)) and ($F_4C_6$-HC═N-1-$C_{10}H_6$)Co(H)$(PMe_3)_2$ (**8**) *via* selective C–F/C–H bond activation. Penta-coordinate dicarbonyl cobalt(I) complexes (2,4,5-$R_1$,$R_2$,$R_3$-$C_6$H-HC═N-1-$C_{10}H_7$)Co$(CO)_2(PMe_3)$ ($R_1$ = F, $R_2$ = H, $R_3$ = F (**9**); $R_1$ = F, $R_2$ = F, $R_3$ = F (**10**)) were obtained from reactions of hexa-coordinate cobalt(III) complexes **5** and **6** with carbon monoxide through reductive elimination. Cobalt(III) halides (2,4,5-$R_1$,$R_2$,$R_3$-$C_6$H-HC═N-1-$C_{10}H_6$)Co(I)$(PMe_3)_2$ ($R_1$ = F, $R_2$ = F, $R_3$ = H (**11**); $R_1$ = F, $R_2$ = H, $R_3$ = F (**12**); $R_1$ = F, $R_2$ = F, $R_3$ = F (**13**)) and (2,4,5-$R_1$,$R_2$,$R_3$-$C_6$H-HC═N-1-$C_{10}H_6$)Co(Br)$(PMe_3)_2$ ($R_1$ = F, $R_2$ = F, $R_3$ = H (**14**); $R_1$ = F, $R_2$ = H, $R_3$ = F (**15**); $R_1$ = F, $R_2$ = F, $R_3$ = F (**16**)) were prepared by the interaction between hydrido cobalt(III) complexes **4–6** and MeI or EtBr. The molecular configurations of complexes **4**, **8**, and **11** were determined by single crystal X-ray diffraction. We then confirmed that the four hydrido cobalt(III) complexes **4–6** and **8** could be used as catalysts for reduction of aldehydes and ketones. Complex **8** is the best catalyst among the four complexes and can selectively catalyze the carbonyl groups of α,β-unsaturated aldehydes and ketones.

Received 15th June 2018,
Accepted 6th August 2018

DOI: 10.1039/c8nj02979b

rsc.li/njc



## Introduction

Recently, great progress has been made on transition-metal-induced C–H bond activation and functionalization because this method provides a green and sustainable way to various new organic compounds. In many reactions, chemists mainly use the second and third transitional series of precious metals. The C–H bond functionalization catalyzed by more abundant and cost-efficient 3d metals, such as Fe, Co, and Ni, is used less. Ackermann summarized stoichiometric and catalytic cobalt-induced C–H bond activation and functionalization.[1] Glorius evaluated a Co-based catalytic system with mild C–H bond activation.[2] The C–H functionalization has been an efficient method for selective derivatization of C–H bonds and has been broadly used in synthetic chemistry.[3] At the same time, more and more fluorinated compounds are being applied in agrochemicals, drugs, and new materials. Not only the formation of C–F bonds, but also the activation of C–F bonds, has been used to prepare organic fluorides because selective defluorinated reactions of per- or polyfluorinated compounds are applicable to syntheses of partially fluorinated compounds. This strategy is often better than direct fluorination since it is not easy to control selectivity using direct fluorination.[4] C–F bond activation of aliphatic fluorides by Lewis acids, Brønsted superacids, and hydrogen bonding or metal complexes provides new methodologies for synthesis of new fluorinated building blocks.[5]

If there are both C–F and C–H bonds within a molecule, it is a selective problem to give priority to C–F or C–H activation when a metal center interacts with the molecule. Although the average bond energy of a C–H bond is smaller than that of a C–F bond, bond energy will vary when the chemical bond is

[a] School of Chemistry and Chemical Engineering, Key Laboratory of Special Functional Aggregated Materials, Ministry of Education, Shandong University, Shanda Nanlu 27, 250100 Jinan, People's Republic of China. E-mail: xli63@sdu.edu.cn
[b] College of Chemistry and Chemical Engineering, Northwest Normal University, 730070 Lanzhou, P. R. China
[c] Institut für Nanotechnologie (INT) und Karlsruher Nano-Micro-Facility (KNMF), Karlsruher Institut für Technologie (KIT), Hermann-von-Helmholtz-Platz 1, 76344 Eggenstein-Leopoldshafen, Germany

† Electronic supplementary information (ESI) available: Table of selected crystallographic data, original IR, $^1$H NMR and $^{19}$F NMR spectra of the compounds and CIF files. CCDC 1840080–1840082. For ESI and crystallographic data in CIF or other electronic format see DOI: 10.1039/c8nj02979b

within a specific molecule. The priority of C–F/C–H bond activation is related to many factors, such as the kind of metal center, its oxidation state, coordination number, spatial configuration, and type of supporting ligands in the metal complex.[6] Therefore, selective activation of a C–F/C–H bond is still a great challenge.

In 2010, we studied the competitive cleavage of a C–F or C–H bond with an imine or carbonyl group as an anchoring group and found that both the anchoring group and the valence of the cobalt atom effect the preference of C–F/C–H bond activation.[7] A similar conclusion was drawn from the reactions of fluorinated imines with $Fe(PMe_3)_4$.[8] The experimentally observed C–F and C–H cyclometalation products by cobalt complexes were rationalized by analyzing the thermodynamic and kinetic properties of C–H and C–F activation pathways.[9] A further investigation of the reactions of different 2,6-difluorophenylarylimines with $Fe(PMe_3)_4$ indicates that C–H bond activation products were obtained if the aryl rings of fluoroarylimines were substituted by electron-withdrawing groups. And, C–F bond activation products were formed if aromatic rings of fluoroarylimines were substituted by electron-donating groups. Surprisingly, both the C–H and C–F bond activation products are hydrido iron complexes.[10] The reaction of $Fe(PMe_3)_4$ with 2,3,5,6-tetrafluoropyridine in pentane selectively resulted in the C–H bond activation product with the release of hydrogen.[11] Fluoroarylimine-stabilized iron hydrides formed *via* selective C–F/C–H bond activation could be used for activating $CO_2$ and $CS_2$[12] and the activation preference of the C–F/C–H bond could be changed with an auxiliary strong Lewis acid.

As a continuation in the field of selective C–F/C–H bond activation, in this work, we have realized selective activation of the C–F and C–H bond from a reaction of $CoMe(PMe_3)_4$ with polyfluorinated aryl imines. Four hydrido [CNC]-pincer cobalt complexes were synthesized and characterized and the properties and catalytic activities of these cobalt hydrides were explored. The cobalt hydrides showed excellent catalytic activity in the hydrosilylation of aldehydes, especially for selective hydrosilylation of the carbonyl groups of α,β-unsaturated aldehydes and ketones.

## Results and discussion

### Selective C–F/C–H bond activation

In order to study selective C–F/C–H bond activation in a phenyl ring, reactions of fluorophenylimines **1–3**[13] with $CoMe(PMe_3)_4$ were carried out to afford hydrido bischelate [CNC]-pincer cobalt(III) complexes **4–6** *via* dual C–H bond activation with the release of a $CH_4$ molecule (eqn (1)). In this process, no *ortho*-(C–F) bond activation was observed. We think that the first step of reaction (1) is *ortho*-(C–H) bond activation of the phenyl ring because this C–H bond activation is easier than activation of the C–H bond at the 8-position of the naphthyl group. This is caused by the F atoms in the phenyl ring. The formation of $CH_4$ and cyclometalation are the driving forces. Activation of a C–H bond at the 8-position of the naphthyl group gives rise to a Co–H bond with formation of a second 5-membered chelate ring.

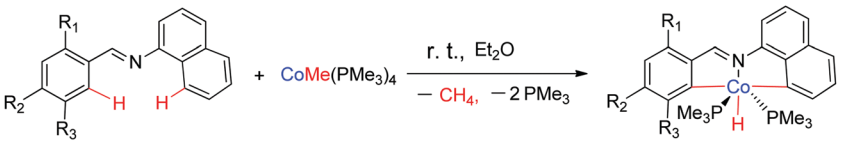


1 - 3 4 - 6 (1)

| | R1 | R2 | R3 |
|---|---|---|---|
| 1 4 | F | F | H |
| 2 5 | F | H | F |
| 3 6 | F | F | F |

In the IR spectra of complexes **4–6**, typical Co–H stretching bands at 1889 (**4**), 1892 (**5**), and 1894 (**6**) $cm^{-1}$ were found. The hydrido resonances of complexes **4–6** were recorded at −18.88 (**4**), −17.75 (**5**), and −17.90 (**6**) ppm as triplets with a coupling constant $J$(PH) = 69.0 Hz in the $^1$H NMR spectra of complexes **4–6**. The singlets at 9.17 (**4**), 9.27 (**5**), and 9.10 (**6**) ppm belong to the hydrogen atoms of the imine groups. In the $^{19}$F NMR spectra of complexes **4–6**, the coupling patterns are in accord with structural characteristics of the corresponding complexes. One signal at 10.4 (**4**), 11.2 (**5**), and 10.5 (**6**) ppm for two $PMe_3$ ligands was registered in the $^{31}$P NMR spectra of complexes **4–6**. This demonstrates that two P atoms in each complex have the same chemical environment in the molecular structure of the complex.

Red crystals of complex **4** suitable for single crystal X-ray diffraction were obtained from its *n*-pentane solution at 0 °C. The molecular structure of complex **4** has a hexa-coordinate configuration (Fig. 1). It is clear that two trimethylphosphine ligands are symmetrical about the [CNC]-pincer plane. This result confirms that the conclusion drawn from the $^{31}$P NMR spectra is correct. Both the phenyl and the naphthyl ring are in the chelate plane. If P1–Co1–P2 (161.11(2)°) is alleged to be axial, then the other four coordination atoms [H100C7C13N1] are in the equatorial plane. Co1–H100 (1.41(2) Å) is in the region of the known Co–H bonds (1.40–1.50 Å).[14] The sum of the four coordination bond angles (N1–Co1–C7 = 83.40(7); C7–Co1–H100 = 99.3(10); H100–Co1–C13 = 94.8(10), and C13–Co1–N1 = 82.48(7)°) around the central cobalt atom in the equatorial plane is 359.98°. This shows that coplanarity of the coordination atoms and Co atom is very good.

The combination of pre-ligand **7** and $CoMe(PMe_3)_4$ (or $Co(PMe_3)_4$) in diethyl ether gave rise to the hydrido [CNC]-pincer cobalt complex **8** *via* both C–F and C–H bond activation with the formation of MeF (or $F_2PMe_3$ in the case of $Co(PMe_3)_4$) (eqn (2)).

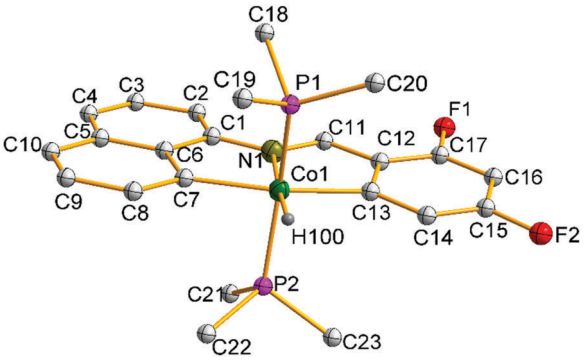


Fig. 1 Molecular structure of complex **4** (most of the hydrogen atoms were omitted for clarity). Selected bond distances (Å) and angle (°): Co1–N1 1.9306(15), Co1–C13 1.9416(17), Co1–C7 1.9661(18), Co1–P2 2.1619(6), Co1–P1 2.1637(6), Co1–H100 1.41(2), N1–C11 1.303(2); N1–Co1–C13 82.48(7), N1–Co1–C7 83.40(7), C13–Co1–C7 165.87(8), N1–Co1–P2 100.17(5), C13–Co1–P2 94.24(5), C7–Co1–P2 88.80(5), N1–Co1–P1 98.21(5), C13–Co1–P1 92.47(5), C7–Co1–P1 88.98(5), P2–Co1–P1 161.11(2), N1–Co1–H100 177.1(10), C13–Co1–H100 94.8(10), C7–Co1–H100 99.3(10), P2–Co1–H100 81.0(11), and P1–Co1–H100 80.9(11).

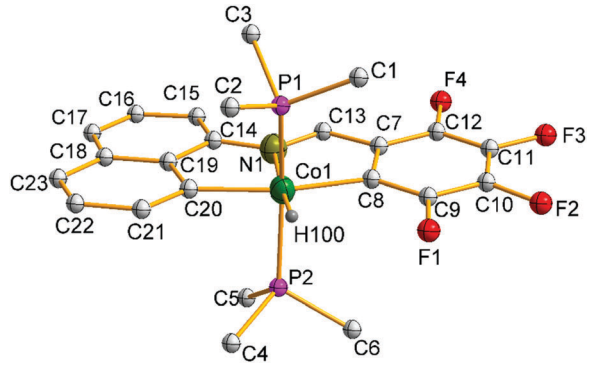


Fig. 2 Molecular structure of complex **8** (most of the hydrogen atoms were omitted for clarity). Selected bond distances (Å) and angle (°): Co1–N1 1.936(2), Co1–C8 1.953(3), Co1–C20 1.965(3), Co1–P1 2.1666(11), Co1–P2 2.1674(12), Co1–H100 1.33(3), N1–C13 1.295(3); N1–Co1–C8 81.75(10), N1–Co1–C20 83.54(10), C8–Co1–C20 165.26(12), N1–Co1–P1 99.01(6), C8–Co1–P1 92.53(8), C20–Co1–P1 89.04(8), N1–Co1–P2 100.60(6), C8–Co1–P2 95.12(8), C20–Co1–P2 88.29(7), P1–Co1–P2 159.78(3), N1–Co1–H100 174.3(11), C8–Co1–H100 94.3(11), C20–Co1–H100 100.3(11), and P1–Co1–H100 77.0(12), P2–Co1–H100 83.8(12).


(2)

MeF and $F_2PMe_3$ in solution could be confirmed by *in situ* $^{19}F$ and $^{31}P$ NMR.[15,16] The $\nu$(Co–H) band in the IR spectrum of complex **8** was recorded at 1893 $cm^{-1}$. The hydrido hydrogen was found at −17.86 ppm as a triplet with a coupling constant of 69.0 Hz while the signal of imine hydrogen was registered at 8.97 ppm as a singlet in the $^1H$ NMR spectrum of complex **8.** In the $^{19}F$ NMR spectrum of complex **8,** there are four groups of F signals with the same integral intensity. This implies that one C–F bond of the five C–F bonds in **7** was cleaved.

Single crystal X-ray diffraction confirmed that complex **8** is hexa-coordinate with an octahedral geometry (Fig. 2). The structural characteristics of cobalt complex **8** are similar to those of complex **4.**

We have known that the reaction of $CoMe(PMe_3)_4$ with an imine derived from 2,6-difluorobenzaldehyde and naphthalene-1-amine provides only C–F activation products without C–H bond activation (eqn (3)).[17] This result is similar to the C–Cl bond activation by cobalt complex.[18]

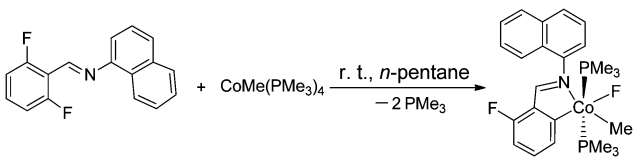


(3)

From the results of eqn (1)–(3) it can be concluded that selective C–F/C–H bond activation is related not only to the location of C–F bonds on the aromatic ring, but also to the number of C–F bonds on the aromatic ring. Based on our early report on C–F/C–H bond activation of polyfluoroaryl imine,[19] we propose a mechanism for reaction (2) (Scheme 1).

The reaction of $CoMe(PMe_3)_4$ with pre-ligand **7** begins with coordination of the N atom of the imine group and the oxidative addition of the C–F bond at the Co(I) center to afford Co(III) intermediate **7A,** an organo cobalt(III) fluoride. The reaction of $Co(PMe_3)_4$ with pre-ligand **7** also starts with coordination of the N atom of the imine group and the oxidative addition of the C–F bond at the Co(0) center to give rise to Co(II) intermediate **7B,** an organo cobalt(II) fluoride. The reductive elimination between Co–Me and Co–F bond of intermediate **7A** delivers intermediate **7C,** a Co(I) species, with the escape of MeF. **7B,** which reacts with $PMe_3$ ligand to give intermediate **7C** and difluorotrimethyl-phosphine, $F_2PMe_3$. After dissociation of one $PMe_3$ ligand, oxidative addition of the C–H bond of the naphthyl group at the unstable Co(I) center of intermediate **7C** generates the final hydrido [CNC]-pincer cobalt(III) complex **8** *via* a second cyclo-metalation. Even though the intermediates **7A, 7B,** and **7C** were not isolated, the existence of these complexes could be indirectly verified by our early work.[17,19]

### Chemical properties of hydrido cobalt(III) complexes 4–6

Hydrido cobalt complexes are important compounds in many fields of synthetic chemistry. Therefore, we further studied the chemical properties of hydrido cobalt complexes. Hydrido cobalt

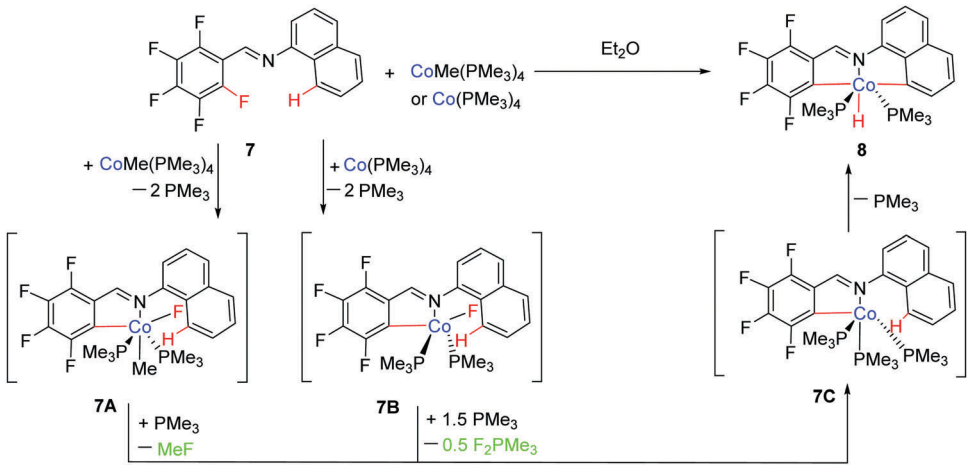


Scheme 1 A proposed mechanism for reaction (2).

complexes **5** and **6** reacted with CO to generate cobalt(I) complexes **9** and **10** (eqn (4)).

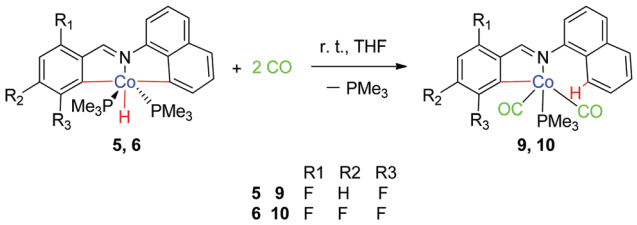


(4)

In the IR spectra of cobalt(I) complexes **9** and **10**, two bands for carbonyl ligands at 2019/1934 (**9**) and 1979/1913 (**10**) $cm^{-1}$ were recorded. The Co–H vibrations of complexes **5** and **6** disappeared. When comparing the $^{1}H$ NMR spectra of complexes **9** and **10**, with those of complexes **5** and **6**, one more aromatic hydrogen atom was found. Resonances of the imine hydrogen atom are situated at 8.42 (**9**) and 8.26 (**10**) ppm. The hydrido signals of complexes **5** and **6** in upfield disappeared. In the $^{31}P$ NMR spectra of complexes **9** and **10**, only one singlet for $PMe_3$ at 8.8 (**9**) and 9.2 (**10**) ppm was detected. From this experimental information, it can be concluded that reaction (4) is not a simple replacement of $PMe_3$ by CO.

We consider that the first step is ligand replacement of $PMe_3$ by CO to form intermediate $\mathbf{A_{5,6}}$ (Scheme 2). Intermediate $\mathbf{A_{5,6}}$ as a carbonyl cobalt(III) species is not stable because of the weak π-backbond between cobalt(III) and CO ligands. After reductive elimination between Co–H and Co–$C_{naphthyl}$ occurs it gives rise to stable penta-coordinate dicarbonyl cobalt(I) complexes **9** and **10** with coordination of the second CO ligand. These experimental results show that the ligand has an important influence on the configuration of the complexes.

The C–X bonds of MeI and EtBr are active and can interact with many transition metal complexes. The reactions of MeI and EtBr with hydrido complexes **4–6** were carried out (eqn (5) and (6)).

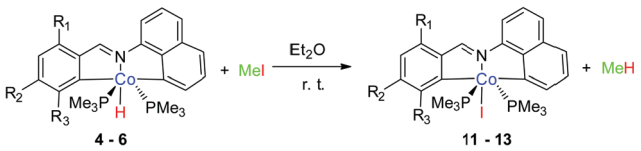


(5)

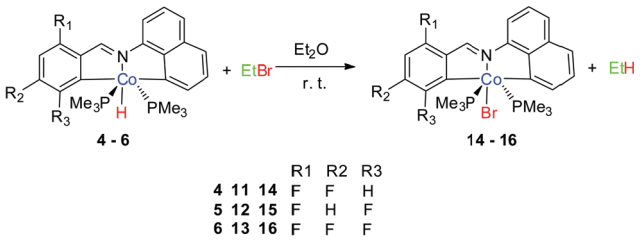


(6)

Complexes **11–13** have similar structures with complexes **14–16**. They are hexa-coordinate di-organo cobalt(III) halides. In the IR spectra of complexes **11–16**, the ν(C═N) vibrations appeared at 1599–1605 $cm^{-1}$. In the $^{1}H$ NMR spectra of complexes **11–16**, the H atom of the imine group was registered at 8.65–9.10 ppm. In the $^{31}P$ NMR spectra of complexes **11–16**, only one singlet was found at 16.3–18.4 ppm. This result shows that

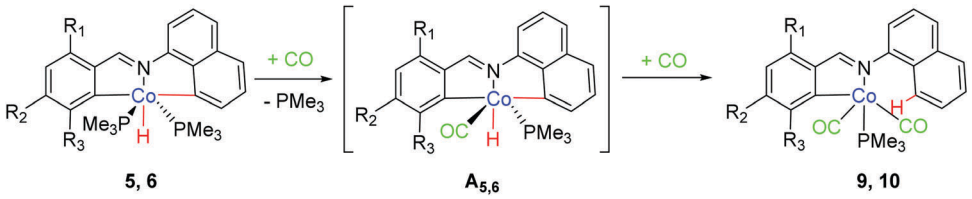


Scheme 2 Pathway of formation of complexes **9** and **10**.

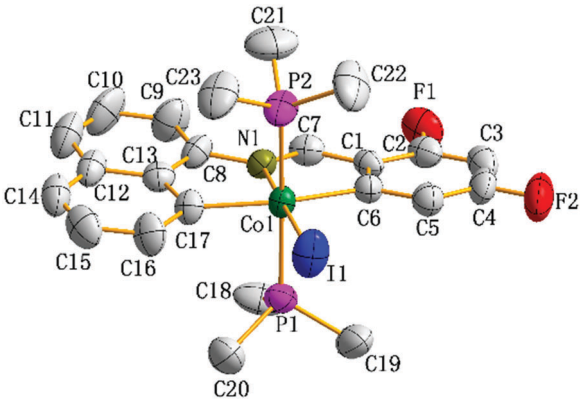


Fig. 3 Molecular structure of complex **11** (all the hydrogen atoms were omitted for clarity). Selected bond distances (Å) and angles (°): I1–Co1 2.6090(8), Co1–N1 1.894(4), Co1–C6 1.957(5), Co1–C17 1.976(5), Co1–P1 2.2210(15), Co1–P2 2.2246(16), N1–C7 1.274(6); N1–Co1–C6 82.47(19), N1–Co1–C17 83.65(19), C6–Co1–C17 166.1(2), N1–Co1–P1 92.43(12), C6–Co1–P1 91.02(15), C17–Co1–P1 88.68(15), N1–Co1–P2 91.13(12), C6–Co1–P2 91.30(15), C17–Co1–P2 89.86(15), P1–Co1–P2 175.98(6), N1–Co1–I1 179.41(13), C6–Co1–I1 97.03(15), C17–Co1–I1 96.86(14), P1–Co1–I1 87.88(4), and P2–Co1–I1 88.58(5).

these two trimethylphosphine ligands are in the same chemical environments. The molecular structure of complex **11** determined by single crystal X-ray diffraction has a hexa-coordinate coordination geometry (Fig. 3). This iodo cobalt(III) complex **11** has the same structural characteristics as its hydrido cobalt(III) complex **4**. Two chelate rings are in the same plane with both the phenyl and naphthyl ring. Two $PMe_3$ ligands are symmetrically placed about the chelate ring, so they have the same chemical environments.

### Catalytic applications of hydrido cobalt complexes 4–6 and 8

It has been reported that hydrido cobalt(III) complexes as catalysts could be used in the reduction of aldehydes and ketones.[20,21] In this work, we found that four hydrido cobalt(III) complexes, **4–6** and **8**, could catalyze the reduction of benzaldehyde to a silyl benzyl ether with silanes as hydrogen sources (Table 1). The control experiment showed that the catalytic reaction did not occur without a catalyst (Table 1, entry 1). Under the same conditions, complex **8** had the best catalytic activity among the four hydrido cobalt complexes (Table 1, entries 2–5). When the

Table 2 Hydrosilylation of aldehydes catalyzed by **8**[a]

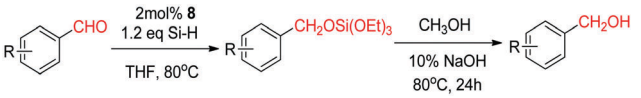


| Entry | Substrate | Conversion[b] (%) | Yield[c] (%) |
|---|---|---|---|
| 1 | 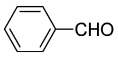 | 99 | 92 |
| 2 | 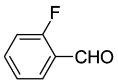 | 92 | 87 |
| 3 | 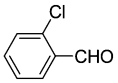 | 90 | 84 |
| 4 | 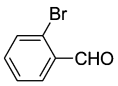 | 85 | 81 |
| 5 | 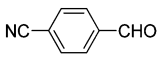 | 83 | 78 |
| 6 | 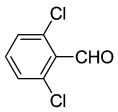 | 92 | 85 |
| 7 | 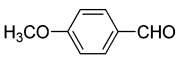 | 87 | 77 |
| 8 | 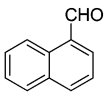 | 93 | 88 |

[a] 2 mol% **8**, $(EtO)_3SiH$, THF, 80 °C, 4 h. [b] GC conversion. [c] Isolated yield.

Table 1 Hydrosilylation of benzaldehyde catalyzed by cobalt hydride under different conditions[a]

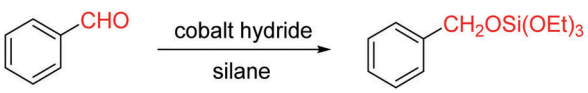


| Entry | Catalyst | Loading (mol%) | Silane | Solvent | Temp. (°C) | Time (h) | Conversion[b] (%) |
|---|---|---|---|---|---|---|---|
| 1 | None | 0 | $(EtO)_3SiH$ | THF | 80 | 24 | 0 |
| 2 | **4** | 2 | $(EtO)_3SiH$ | THF | 80 | 4 | 71 |
| 3 | **5** | 2 | $(EtO)_3SiH$ | THF | 80 | 4 | 67 |
| 4 | **6** | 2 | $(EtO)_3SiH$ | THF | 80 | 4 | 80 |
| 5 | **8** | 2 | $(EtO)_3SiH$ | THF | 80 | 4 | 99 |
| 6 | **8** | 2 | $(EtO)_3SiH$ | THF | 80 | 2 | 85 |
| 7 | **8** | 1 | $(EtO)_3SiH$ | THF | 80 | 4 | 76 |
| 8 | **8** | 2 | $(EtO)_3SiH$ | THF | 60 | 4 | 68 |
| 9 | **8** | 2 | $(EtO)_3SiH$ | THF | 50 | 4 | 54 |
| 10 | **8** | 2 | $(EtO)_3SiH$ | THF | 30 | 4 | 11 |
| 11 | **8** | 2 | $Et_3SiH$ | THF | 80 | 4 | 24 |
| 12 | **8** | 2 | $Ph_3SiH$ | THF | 80 | 4 | 0 |
| 13 | **8** | 2 | $Me(EtO)_2SiH$ | THF | 80 | 4 | 59 |
| 14 | **8** | 2 | $(EtO)_3SiH$ | Toluene | 80 | 4 | 88 |

[a] Reaction conditions: PhCHO (1.0 mmol), $R_3SiH$ (1.2 mmol), solvent (2 mL). [b] Determined by GC with *n*-dodecane as an internal standard.

reaction temperature was lower than 80 °C, the conversion became low (Table 1, entries 8–10). It was found that $(EtO)_3SiH$ is the best hydrogen source among the tested four silanes (Table 1, entries 5 and 11–13). If the catalyst loading was decreased to 1 mol%, then the conversion became 76% from 99% (Table 1, entries 5 and 7). If the reaction time was shortened to 2 hours, then the conversion decreased to 85% (Table 1, entry 6). We also confirmed that THF is a better reaction medium than toluene for this catalytic reaction (Table 1, entries 5 and 14).

To expand the scope of the substrates, more aldehydes were tested under the optimized conditions: 2 mol% catalyst loading, $(EtO)_3SiH$, THF, 4 h, 80 °C (Table 2). Whether the phenyl group of the substrate has an electron-withdrawing group or electron-donating group, the catalytic reaction could take place and the isolated yields were between 77–92%. With 1-naphthaldehyde as substrate, the conversion reached 93% and the isolated yield was 88%. In general, ketones are less active than aldehydes for these reduction reactions. Some aromatic ketones were selected as substrates for this catalytic system (Table 3, entries 1–5). The results show that both conversions and the isolated yields are lower than those with the aldehydes (Table 2). The conversion of an aliphatic ketone is significantly lower than that of an aromatic ketone (Table 3, entries 6 and 7). Interestingly, α,β-unsaturated aldehydes could selectively transfer to the corresponding α,β-unsaturated alcohols (Table 4, entries 1–5). In this process, the C=C bond remained unchanged. Under the catalytic conditions, chalcone transformed to 1,3-diphenyl-pro-2-en-1-ol in an isolated yield of 87% with a conversion of 94%. In comparison with the data in Table 3, it can be concluded that an α,β-unsaturated ketone is more active than a normal ketone.

Table 3 Hydrosilylation of ketones catalyzed by **8**[a]

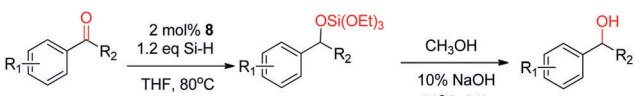


| Entry | Substrate | Conversion[b] (%) | Yield[c] (%) |
|---|---|---|---|
| 1 | 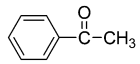 | 85 | 77 |
| 2 | 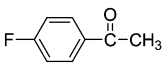 | 88 | 78 |
| 3 | 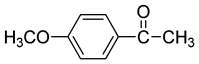 | 77 | 70 |
| 4 | 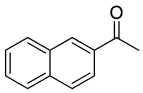 | 85 | 75 |
| 5 |  | 82 | 72 |
| 6 |  | 60 | 57[d] |
| 7 |  | 76 | 71[d] |

[a] 2 mol% **8**, $(EtO)_3SiH$, THF, 80 °C, 4 h. [b] GC conversion. [c] Isolated yield. [d] GC yield.

Table 4 Selective reduction of α,β-unsaturated carbonyls catalyzed by **8**[a]

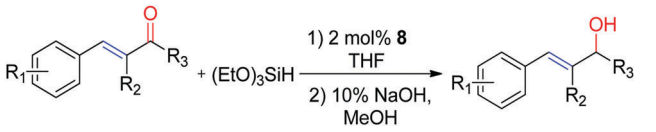


| Entry | Substrate | Conversion[b] (%) | Yield[c] (%) |
|---|---|---|---|
| 1 | 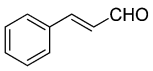 | 91 | 85 |
| 2 | 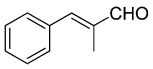 | 85 | 80 |
| 3 | 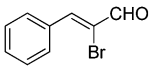 | 58 | 55 |
| 4 | 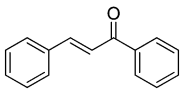 | 96 | 86 |
| 5 | 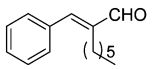 | 95 | 88 |
| 6 | 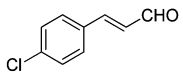 | 94 | 87 |

[a] Cinnamaldehyde (1.0 mmol), $(EtO)_3SiH$ (1.2 mmol), **8** (0.02 mmol) in 2 mL THF, 80 °C, 4 h. [b] GC conversion. [c] Isolated yield.

## Conclusions

Hydrido [CNC]-pincer cobalt(III) complexes **4–6** and **8** were prepared from reactions of polyfluorinated aryl imines **1–3** and **7** with $CoMe(PMe_3)_4$ *via* selective C–H/C–F bond activation. Hydrido complexes **5** and **6** reacted with CO to give rise to dicarbonyl cobalt(I) complexes **9** and **10** *via* reductive elimination and in this process the hexa-coordinate cobalt(III) complexes transformed to penta-coordinate cobalt(I) complexes. Complexes **4–6** interacted with MeI or EtBr afforded iodo cobalt(III) complexes **11–13** or bromo cobalt(III) complexes **14–16**. The molecular structures of complexes **4**, **8**, and **11** were determined by single crystal X-ray diffraction. It was found that these four hydrido cobalt(III) complexes **4–6** and **8** could catalyze the reduction reactions of aldehydes and ketones. Among them, complex **8** has the strongest catalytic activity. Complex **8** selectively catalyzed the carbonyl group of α,β-unsaturated aldehydes and ketone with an unchanged C=C bond.

## Experimental section

### General procedures and materials

Standard vacuum techniques were applied to the preparation of all air-sensitive materials in this paper. Solvents were dried with sodium on the basis of known procedures and distilled in nitrogen atmosphere before use. Schiff bases were prepared by

 

condensation of polyfluorobenzaldehyde with amines by refluxing in alcohol solution. $CoMe(PMe_3)_4$ and $Co(PMe_3)_4$ were prepared according to literature methods.[22] Infrared spectra (4000–400 $cm^{-1}$) were obtained with a Bruker ALPHA FT-IR instrument used with Nujol mulls between KBr disks to display the characteristic peaks of substances. NMR data were recorded on a Bruker Avance 300 MHz spectrometer. GC was collected with a Fuli 9790 instrument with *n*-dodecane as an internal standard. All the aldehydes and ketones were purchased and some of them were freshly distilled before use.

**Preparation of complex 4.** A solution of imine **1** (0.54 g, 2.0 mmol) in 20 mL of diethyl ether was added into a solution of $CoMe(PMe_3)_4$ (0.95 g, 2.5 mmol) in 40 mL of diethyl ether at −78 °C. After stirring for 24 h at room temperature, the reaction mixture turned red. Then the diethyl ether was transferred, and *n*-pentane was used to extract the residual solid. After filtering, the product (0.67 g, 72% yield) was obtained as red crystals from *n*-pentane at 0 °C. Dec. >135 °C. IR (Nujol mull, KBr, $cm^{-1}$): 1889 $\nu$(Co–H), 1559 $\nu$(C═N), 1528 $\nu$(C═C), 942 $\rho(PMe_3)$. $^1$H NMR (300 MHz, $C_6D_6$, 298 K, $\delta$/ppm): 9.17 (s, 1H, C*H*═N), 7.59–7.16 (m, 7H, Ar-*H*), 6.49 (t, $J$ = 9.0 Hz, 1H, Ar-*H*), 0.53 (s, 18H, P*Me*$_3$), −18.88 (t, $J$ = 69.0 Hz, 1H, Co-*H*). $^{31}$P NMR (121 MHz, $C_6D_6$, 298 K, $\delta$/ppm): 10.4 (s, *P*Me$_3$). $^{19}$F NMR (282 MHz, $C_6D_6$, 298 K, $\delta$/ppm): −108.7 (d, $J$ = 8.5 Hz, 1F), −113.0 (d, $J$ = 8.5 Hz, 1F). Anal. calc. For $C_{23}H_{28}CoF_2NP_2$ (477.35 g $mol^{-1}$): C, 57.87; H, 5.91; N, 2.93. Found: C, 57.74; H, 5.95; N, 2.88.

**Preparation of complex 5.** A solution of imine **2** (0.54 g, 2.0 mmol) in 20 mL of diethyl ether was added to a solution of $CoMe(PMe_3)_4$ (0.95 g, 2.5 mmol) in 40 mL of diethyl ether at −78 °C. After stirring for 24 h at room temperature, the reaction mixture turned red. Then the diethyl ether was transferred, and *n*-pentane was used to extract the residual solid. After filtering, the product (0.73 g, 78% yield) was obtained as red crystals from the *n*-pentane at 0 °C. Dec. >135 °C. IR (Nujol mull, KBr, $cm^{-1}$): 1892 $\nu$(Co–H), 1600 $\nu$(C═N), 1539 $\nu$(C═C), 942 $\rho(PMe_3)$. $^1$H NMR (300 MHz, $C_6D_6$, 298 K, $\delta$/ppm): 9.27 (s, 1H, C*H*═N), 7.68–7.32 (m, 4H, Ar-*H*), 7.15–6.52 (m, 4H, Ar-*H*), 0.61 (t, $J$ = 3.0 Hz, 18H, P*Me*$_3$), −17.77 (t, $J$ = 69.0 Hz, 1H, Co-*H*). $^{31}$P NMR (121 MHz, $C_6D_6$, 298K, $\delta$/ppm): 11.2 (s, *P*Me$_3$). $^{19}$F NMR (282 MHz, $C_6D_6$, 298 K, $\delta$/ppm): −97.3 (d, $J$ = 25.4 Hz, 1F), −122.2 (d, $J$ = 25.4 Hz, 1F). Anal. calc. For $C_{23}H_{28}CoF_2NP_2$ (477.35 g $mol^{-1}$): C, 57.87; H, 5.91; N, 2.93. Found: C, 57.77; H, 5.89; N, 2.80.

**Preparation of complex 6.** A solution of imine **3** (0.57 g, 2.0 mmol) in 20 mL of diethyl ether was added to a solution of $CoMe(PMe_3)_4$ (0.95 g, 2.5 mmol) in 40 mL of diethyl ether at −78 °C. After stirring for 24 h at room temperature, the reaction mixture turned red. Then the diethyl ether was transferred, and *n*-pentane was used to extract the residual solid. After filtering, the product (0.84 g, 85% yield) was obtained as red crystals from the *n*-pentane at 0 °C. Dec. >167 °C. IR (Nujol mull, KBr, $cm^{-1}$): 1894 $\nu$(Co–H), 1602 $\nu$(C═N), 1527 $\nu$(C═C), 940 $\rho(PMe_3)$. $^1$H NMR (300 MHz, $C_6D_6$, 298 K, $\delta$/ppm): 9.10 (s, 1H, C*H*═N), 7.59–7.28 (m, 4H, Ar-*H*), 7.16–7.12 (m, 2H, Ar-*H*), 6.54–6.46 (m, 1H, Ar-*H*), 0.64 (s, 18H, P*Me*$_3$), −17.90 (t, $J$ = 69.0 Hz, 1H, Co-*H*). $^{31}$P NMR (121 MHz, $C_6D_6$, 298 K, $\delta$/ppm): 10.5 (s, *P*Me$_3$). $^{19}$F NMR (282 MHz, $C_6D_6$, 298 K, $\delta$/ppm): −117.5 (d, $J$ = 22.6 Hz, 1F), −120.9 (dd, $J$ = 30.0, 22.6 Hz, 1F), −131.0 (d, $J$ = 30.0 Hz, 1F). Anal. calc. For $C_{23}H_{27}CoF_3NP_2$ (495.34 g $mol^{-1}$): C, 54.77; H, 5.49; N, 2.83. Found: C, 55.82; H, 5.48; N, 2.74.

**Preparation of complex 8.** A solution of imine **7** (0.64 g, 2.0 mmol) in 20 mL of diethyl ether was added to a solution of $CoMe(PMe_3)_4$ (0.95 g, 2.5 mmol) or $Co(PMe_3)_4$ (0.91 g, 2.5 mmol) in 40 mL of diethyl ether at −78 °C. After stirring for 24 h at room temperature, the reaction mixture turned red. Then the diethyl ether was transferred, and *n*-pentane was used to extract the residual solid. After filtering, the product (0.48 g, 47% yield) was obtained as red crystals from the *n*-pentane at 0 °C. Dec. >280 °C. IR (Nujol mull, KBr, $cm^{-1}$): 1893 $\nu$(Co–H), 1628 $\nu$(C═N), 1599, 1531 $\nu$(C═C), 940 $\rho(PMe_3)$. $^1$H NMR (300 MHz, $C_6D_6$, 298 K, $\delta$/ppm): 8.97 (s, 1H, C*H*═N), 7.59–7.27 (m, 4H, Ar-*H*), 7.13–7.06 (m, 2H, Ar-*H*), 0.50 (t, $J$ = 3.0 Hz, 18H, P*Me*$_3$), −17.86 (t, $J$ = 69.0 Hz, 1H, Co-*H*). $^{31}$P NMR (121 MHz, $C_6D_6$, 298 K, $\delta$/ppm): 10.9 (s, *P*Me$_3$). $^{19}$F NMR (282 MHz, $C_6D_6$, 298 K, $\delta$/ppm): −116.2 (dd, $J$ = 22.6, 19.7 Hz, 1F), −141.2 (t, $J$ = 19.7 Hz, 1F), −153.4 (dd, $J$ = 33.8, 19.7 Hz, 1F), −164.6 (t, $J$ = 19.7 Hz, 1F). Anal. calc. For $C_{23}H_{26}CoF_4NP_2$ (513.33 g $mol^{-1}$): C, 53.81; H, 5.11; N, 2.73. Found: C, 53.73; H, 5.08; N, 2.82.

**Preparation of complex 9.** CO (1 bar) was bubbled into a solution of complex **5** (0.48 g, 1.0 mmol) in 40 mL of THF. After stirring for 48 h at room temperature, the reaction mixture turned light red. Then the THF was transferred, and *n*-pentane was used to extract the residual solid. After filtering, the product (0.29 g, 63% yield) was obtained as yellowish red crystals from the *n*-pentane at 0 °C. Dec. >258 °C. IR (Nujol mull, KBr, $cm^{-1}$): 2019, 1934 $\nu$(C═O), 1614 $\nu$(C═N), 1543 $\nu$(C═C), 946 $\rho(PMe_3)$. $^1$H NMR (300 MHz, $C_6D_6$, 298 K, $\delta$/ppm): 8.42 (s, 1H, C*H*═N), 7.67 (d, $J$ = 6.0 Hz, 1H, Ar-*H*), 7.54 (d, $J$ = 6.0 Hz, 1H, Ar-*H*), 7.42 (d, $J$ = 9.0 Hz, 1H, Ar-*H*), 7.16 (m, 1H, Ar-*H*), 7.10–6.99 (m, 2H, Ar-*H*), 6.77 (m, 1H, Ar-*H*), 6.61 (d, $J$ = 9.0 Hz, 1H, Ar-*H*), 6.52–6.45 (m, 1H, Ar-*H*), 0.43 (d, $J$ = 9.0 Hz, 9H, P*Me*$_3$). $^{31}$P NMR (121 MHz, $C_6D_6$, 298 K, $\delta$/ppm): 8.8 (s, *P*Me$_3$). $^{19}$F NMR (282 MHz, $C_6D_6$, 298 K, $\delta$/ppm): −100.1 (s, 1F), −120.7 (s, 1F). Anal. calc. For $C_{22}H_{19}CoF_2NO_2P$ (457.30 g $mol^{-1}$): C, 57.78; H, 4.19; N, 3.06. Found: C, 57.87; H, 4.29; N, 3.04.

**Preparation of complex 10.** CO (1 bar) was bubbled into a solution of complex **6** (0.50 g, 1.0 mmol) in 40 mL of THF. After stirring for 48 h at room temperature, the reaction mixture turned light red. Then the THF was transferred, and *n*-pentane was used to extract the residual solid. After filtering, the product (0.27 g, 56% yield) was obtained as yellowish red crystals from the *n*-pentane at 0 °C. Dec. >136 °C. IR (Nujol mull, KBr, $cm^{-1}$): 1979, 1913 $\nu$(C═O), 1614 $\nu$(C═N), 1540 $\nu$(C═C), 951 $\rho(PMe_3)$. $^1$H NMR (300 MHz, $C_6D_6$, 298 K, $\delta$/ppm): 8.26 (s, 1H, C*H*═N), 7.66 (d, $J$ = 9.0 Hz, 1H, Ar-*H*), 7.56 (d, $J$ = 9.0 Hz, 1H, Ar-*H*), 7.43 (d, $J$ = 6.0 Hz, 1H, Ar-*H*), 7.21–7.17 (m, 1H, Ar-*H*), 7.13–7.01 (m, 2H, Ar-*H*), 6.55 (d, $J$ = 24.0 Hz, 1H, Ar-*H*), 6.43–6.34 (m, 1H, Ar-*H*), 0.41 (d, $J$ = 9.0 Hz, 9H, P*Me*$_3$). $^{31}$P NMR (121 MHz, $C_6D_6$, 298 K, $\delta$/ppm): 9.2 (s, *P*Me$_3$). $^{19}$F NMR (282 MHz, $C_6D_6$, 298 K, $\delta$/ppm): −115.4 (d, $J$ = 19.7 Hz, 1F), −123.4 to −123.6 (m, 1F),

−129.8 (d, $J$ = 25.4 Hz, 1F). Anal. calc. For $C_{22}H_{18}CoF_3NO_2P$ (475.29 g mol$^{-1}$): C, 55.60; H, 3.82; N, 2.95. Found: C, 55.52; H, 3.88; N, 2.86.

**Preparation of complex 11.** A solution of MeI (0.22 g, 1.5 mmol) in 10 mL of diethyl ether was added to a solution of complex **4** (0.48 g, 1.0 mmol) in 40 mL of diethyl ether at −78 °C. After stirring for 24 h at room temperature, the reaction mixture turned light red. After filtering, the product (0.39 g, 65% yield) was obtained as light red crystals from the *n*-pentane at 0 °C. Dec. >248 °C. IR (Nujol mull, KBr, cm$^{-1}$): 1599 $\nu$(C═N), 1548, 1528 $\nu$(C═C), 944 $\rho$(PMe$_3$). $^1$H NMR (300 MHz, $C_6D_6$, 298 K, $\delta$/ppm): 8.80–8.74 (m, 2H, C*H*═N and Ar-*H*), 8.61 (t, $J$ = 6.0 Hz, 1H, Ar-*H*), 7.54 (d, $J$ = 9.0 Hz, 1H, Ar-*H*), 7.45 (m, 2H, Ar-*H*), 7.01 (t, $J$ = 9.0 Hz, 1H, Ar-*H*), 6.76 (d, $J$ = 9.0 Hz, 1H, Ar-*H*), 6.52–6.45 (m, 1H, Ar-*H*), 0.61 (t, $J$ = 6.0 Hz, 18H, P*Me*$_3$). $^{31}$P NMR (121 MHz, $C_6D_6$, 298 K, $\delta$/ppm): 16.3 (s, *P*Me$_3$). $^{19}$F NMR (282 MHz, $C_6D_6$, 298 K, $\delta$/ppm): −103.7 (d, $J$ = 8.5 Hz, 1F), −112.0 (d, $J$ = 8.5 Hz, 1F). Anal. calc. For $C_{23}H_{27}CoF_2INP_2$ (603.25 g mol$^{-1}$): C, 45.79; H, 4.51; N, 2.32. Found: C, 45.57; H, 4.48; N, 2.46.

**Preparation of complex 12.** A solution of MeI (0.22 g, 1.5 mmol) in 10 mL of diethyl ether was added to a solution of complex **5** (0.48 g, 1.0 mmol) in 40 mL of diethyl ether at −78 °C. After stirring for 24 h at room temperature, the reaction mixture turned light red. After filtering, the product (0.36 g, 59% yield) was obtained as light red crystals from the *n*-pentane at 0 °C. Dec. >273 °C. IR (Nujol mull, KBr, cm$^{-1}$): 1599 $\nu$(C═N), 1575, 1540 $\nu$(C═C), 941 $\rho$(PMe$_3$). $^1$H NMR (300 MHz, $C_6D_6$, 298 K, $\delta$/ppm): 9.10–9.07 (m, 1H, C*H*═N), 8.66 (t, $J$ = 6.0 Hz, 1H, Ar-*H*), 7.55–7.43 (m, 3H, Ar-*H*), 6.97 (t, $J$ = 9.0 Hz, 1H, Ar-*H*), 6.85–6.79 (m, 1H, Ar-*H*), 6.70 (d, $J$ = 9.0 Hz, 1H, Ar-*H*), 6.55–6.49 (m, 1H, Ar-*H*), 0.78 (t, $J$ = 6.0 Hz, 18H, P*Me*$_3$). $^{31}$P NMR (121 MHz, $C_6D_6$, 298 K, $\delta$/ppm): 17.5 (s, *P*Me$_3$). $^{19}$F NMR (282 MHz, $C_6D_6$, 298 K, $\delta$/ppm): −90.4 (d, $J$ = 22.5 Hz, 1F), −121.5 (d, $J$ = 22.6 Hz, 1F). Anal. calc. For $C_{23}H_{27}CoF_2INP_2$ (603.25 g mol$^{-1}$): C, 45.79; H, 4.51; N, 2.32. Found: C, 45.68; H, 4.45; N, 2.27.

**Preparation of complex 13.** A solution of MeI (0.22 g, 1.5 mmol) in 10 mL of diethyl ether was added to a solution of complex **6** (0.50 g, 1.0 mmol) in 40 mL of diethyl ether at −78 °C. After stirring for 24 h at room temperature, the reaction mixture turned light red. After filtering, the product (0.48 g, 77% yield) was obtained as light red crystals from the *n*-pentane at 0 °C. Dec. >268 °C. IR (Nujol mull, KBr, cm$^{-1}$): 1605 $\nu$(C═N), 1581, 1534 $\nu$(C═C), 940 $\rho$(PMe$_3$). $^1$H NMR (300 MHz, $C_6D_6$, 298 K, $\delta$/ppm): 9.03–9.00 (m, 1H, C*H*═N), 8.51 (t, $J$ = 3.0 Hz, 1H, Ar-*H*), 7.55–7.43 (m, 3H, Ar-*H*), 6.97 (t, $J$ = 9.0 Hz, 1H, Ar-*H*), 6.67 (d, $J$ = 6.0 Hz, 1H, Ar-*H*), 6.51–6.44 (m, 1H, Ar-*H*), 0.73 (t, $J$ = 6.0 Hz, 18H, P*Me*$_3$). $^{31}$P NMR (121 MHz, $C_6D_6$, 298 K, $\delta$/ppm): 17.4 (s, *P*Me$_3$). $^{19}$F NMR (282 MHz, $C_6D_6$, 298 K, $\delta$/ppm): −115.9 (dd, $J$ = 28.2, 22.6 Hz, 1F), −116.9 (dd, $J$ = 5.6, 22.6 Hz, 1F), −126.1 (dd, $J$ = 28.2, 5.6 Hz, 1F). Anal. calc. For $C_{23}H_{26}CoF_3INP_2$ (621.24 g mol$^{-1}$): C, 44.47; H, 4.22; N, 2.25. Found: C, 44.38; H, 4.48; N, 2.46.

**Preparation of complex 14.** A solution of EtBr (0.16 g, 1.5 mmol) in 10 mL of diethyl ether was added to a solution of complex **4** (0.48 g, 1.0 mmol) in 40 mL of diethyl ether at −78 °C. After stirring for 24 h at room temperature, the reaction mixture turned light red. After filtering, the product (0.38 g, 69% yield) was obtained as light red crystals from the *n*-pentane at 0 °C. Dec. >240 °C. IR (Nujol mull, KBr, cm$^{-1}$): 1599 $\nu$(C═N), 1576, 1524 $\nu$(C═C), 943 $\rho$(PMe$_3$). $^1$H NMR (300 MHz, $C_6D_6$, 298 K, $\delta$/ppm): 8.73 (s, 1H, C*H*═N), 8.16 (s, 1H, Ar-*H*), 8.04 (d, $J$ = 9.0 Hz, 1H, Ar-*H*), 7.65 (d, $J$ = 6.0 Hz, 1H, Ar-*H*), 7.44 (m, 3H, Ar-*H*), 7.24–7.23 (m, 1H, Ar-*H*), 6.55 (t, $J$ = 9.0 Hz, 1H, Ar-*H*), 0.73 (s, 18H, P*Me*$_3$). $^{31}$P NMR (121 MHz, $C_6D_6$, 298 K, $\delta$/ppm): 17.3 (s, *P*Me$_3$). $^{19}$F NMR (282 MHz, $C_6D_6$, 298 K, $\delta$/ppm): −104.1 (d, $J$ = 8.5 Hz, 1F), −112.4 (d, $J$ = 8.5 Hz, 1F). Anal. calc. For $C_{23}H_{27}CoF_2BrNP_2$ (556.25 g mol$^{-1}$): C, 49.66; H, 4.89; N, 2.52. Found: C, 49.52; H, 4.78; N, 2.46.

**Preparation of complex 15.** A solution of EtBr (0.16 g, 1.5 mmol) in 10 mL of diethyl ether was added to a solution of complex **5** (0.48 g, 1.0 mmol) in 40 mL of diethyl ether at −78 °C. After stirring for 24 h at room temperature, the reaction mixture turned light red. After filtering, the product (0.35 g, 63% yield) was obtained as light red crystals from the *n*-pentane at 0 °C. Dec. >238 °C. IR (Nujol mull, KBr, cm$^{-1}$): 1601 $\nu$(C═N), 1578, 1541 $\nu$(C═C), 939 $\rho$(PMe$_3$). $^1$H NMR (300 MHz, $C_6D_6$, 298 K, $\delta$/ppm): 8.67 (t, $J$ = 3.0 Hz, 1H, C*H*═N), 8.14–8.10 (m, 1H, Ar-*H*), 7.55 (d, $J$ = 9.0 Hz, 1H, Ar-*H*), 7.37–7.27 (m, 3H, Ar-*H*), 7.16–7.11 (m, 1H, Ar-*H*), 6.88–6.82 (m, 1H, Ar-*H*), 6.66–6.59 (m, 1H, Ar-*H*), 0.73 (t, $J$ = 6.0 Hz, 18H, P*Me*$_3$). $^{31}$P NMR (121 MHz, $C_6D_6$, 298 K, $\delta$/ppm): 18.4 (s, *P*Me$_3$). $^{19}$F NMR (282 MHz, $C_6D_6$, 298 K, $\delta$/ppm): −99.2 (d, $J$ = 22.5 Hz, 1F), −121.7 (d, $J$ = 22.6 Hz, 1F). Anal. calc. For $C_{23}H_{27}CoF_2BrNP_2$ (556.25 g mol$^{-1}$): C, 49.66; H, 4.89; N, 2.52. Found: C, 49.52; H, 4.78; N, 2.46.

**Preparation of complex 16.** A solution of EtBr (0.16 g, 1.5 mmol) in 10 mL of diethyl ether was added to a solution of complex **6** (0.50 g, 1.0 mmol) in 40 mL of diethyl ether at −78 °C. After stirring for 24 h at room temperature, the reaction mixture turned light red. After filtering, the product (0.42 g, 73% yield) was obtained as light red crystals from the *n*-pentane at 0 °C. Dec. >280 °C. IR (Nujol mull, KBr, cm$^{-1}$): 1605 $\nu$(C═N), 1538 $\nu$(C═C), 942 $\rho$(PMe$_3$). $^1$H NMR (300 MHz, $C_6D_6$, 298 K, $\delta$/ppm): 8.68–8.65 (m, 1H, C*H*═N), 8.36 (t, $J$ = 3.0 Hz, 1H, Ar-*H*), 7.55–7.44 (m, 3H, Ar-*H*), 6.97–6.90 (m, 1H, Ar-*H*), 6.62 (d, $J$ = 6.0 Hz, 1H, Ar-*H*), 6.52–6.44 (m, 1H, Ar-*H*), 0.62 (t, $J$ = 6.0 Hz, 18H, P*Me*$_3$). $^{31}$P NMR (121 MHz, $C_6D_6$, 298 K, $\delta$/ppm): 17.8 (s, *P*Me$_3$). $^{19}$F NMR (282 MHz, $C_6D_6$, 298 K, $\delta$/ppm): −117.2 (dd, $J$ = 22.6, 5.6 Hz, 1F), −122.6 (dd, $J$ = 28.2, 22.6 Hz, 1F), −126.4 (dd, $J$ = 28.2, 5.6 Hz, 1F). Anal. calc. For $C_{23}H_{26}CoF_3BrNP_2$ (574.24 g mol$^{-1}$): C, 48.11; H, 4.56; N, 2.44. Found: C, 48.22; H, 4.48; N, 2.46.

**Representative experimental procedure of catalytic reduction of aldehydes and ketones.** A 25 mL Schlenk tube was charged with a mixture of PhCHO (1.0 mmol), HSi(OEt)$_3$ (1.2 mmol) and complex **8** (0.02 mmol) in 2 mL of THF. The reaction vessel was stirred at 80 °C for 4 h and reaction progress was monitored by GC. After cooling to room temperature, $CH_3OH$ (3 mL) and 10% NaOH (5 mL) were added to the tube. After stirring for 24 h at 60 °C, the product was extracted with $Et_2O$ (30 mL × 2). The combined organic phases were dried over anhydrous $Na_2SO_4$, filtered, and the solvent was evaporated under reduced pressure.

 

The product was purified by column chromatography on silica gel (petroleum ether (60–90 °C)/ethyl acetate 5 : 1, v/v) to afford $PhCH_2OH$ as a colorless liquid (0.098 g, 92%).

**Representative experimental procedure of catalytic reduction of α,β-unsaturated aldehydes.** A 25 mL Schlenk tube was charged with a mixture of cinnamaldehyde (1.0 mmol), $HSi(OEt)_3$ (1.2 mmol), and complex **8** (0.02 mmol) in 2 mL of THF. The reaction vessel was stirred at 80 °C for 4 h and the progress of the reaction was monitored by TLC. After cooling to room temperature, $CH_3OH$ (3 mL) and 10% NaOH (5 mL) were added to the tube. After stirring for 24 h at 60 °C, the product was extracted with $Et_2O$ (30 mL × 2). The combined organic phases were dried over anhydrous $Na_2SO_4$, filtered, and the solvent was evaporated under reduced pressure. The product was purified by column chromatography on silica gel (petroleum ether (60–90 °C)/ethyl acetate 3 : 1, v/v) to afford cinnamyl alcohol as pale yellow crystals (0.113 g, 85.0%).

**X-ray crystal structure determinations.** Single crystal X-ray diffraction data of the complexes (**4**, **8**, **11**) were collected on a Bruker SMART Apex II CCD diffractometer equipped with graphite-monochromated Mo Kα radiation ($\lambda$ = 0.71073 Å). During collection of the intensity data, no significant decay was observed. The intensities were corrected for Lorentz-polarization effects and empirical absorption with the SADABS program. The structures were resolved by direct or Patterson methods with the SHELXS-97 program and were refined on $F^2$ with SHELXTL. All non-hydrogen atoms were refined anisotropically. Hydrogen atoms were included in calculated positions and were refined using a riding model. A residual Q peak with peak value greater than 1 around the cobalt center was theoretically defined as a hydrido hydrogen atom. Then the structure was constantly refined and optimized to determine the location of the hydrido hydrogen. CCDC 1840081(**4**), 1840080 (**8**), 1840082 (**11**) contain the supplementary crystallographic data for this paper.†

## Conflicts of interest

There are no conflicts to declare.

## Acknowledgements

This work was supported by the NSF China (no. 21372143).

## References

1 M. Moselage, J. Li and L. Ackermann, *ACS Catal.*, 2016, **6**, 498–525.
2 T. Gensch, M. N. Hopkinson, F. Glorius and J. Wencel-Delord, *Chem. Soc. Rev.*, 2016, **45**, 2900–2936.
3 H. M. L. Davies and D. Morton, *J. Org. Chem.*, 2016, **81**, 343–350.
4 H. Amii and K. Uneyama, *Chem. Rev.*, 2009, **109**, 2119–2183.
5 Q. Shen, Y.-G. Huang, C. Liu, J.-C. Xiao, Q.-Y. Chen and Y. Guo, *J. Fluorine Chem.*, 2015, **179**, 14–22.
6 O. Eisenstein, J. Milani and R. N. Perutz, *Chem. Rev.*, 2017, **117**, 8710–8753.
7 T. Zheng, H. Sun, J. Ding, Y. Zhang and X. Li, *J. Organomet. Chem.*, 2010, **695**, 1873–1877.
8 X. Xu, J. Jia, H. Sun, Y. Liu, W. Xu, Y. Shi, D. Zhang and X. Li, *Dalton Trans.*, 2013, **42**, 3417–3428.
9 J. Li, D. Zhang, H. Sun and X. Li, *Org. Biomol. Chem.*, 2014, **12**, 1897–1907.
10 L. Wang, H. Sun and X. Li, *Eur. J. Inorg. Chem.*, 2015, 2732–2743.
11 T. Zheng, J. Li, S. Zhang, B. Xue, H. Sun, X. Li, O. Fuhr and D. Fenske, *Organometallics*, 2016, **35**, 3538–3545.
12 L. Wang, H. Sun, Z. Zuo, X. Li, W. Xu, R. Langer, O. Fuhr and D. Fenske, *Eur. J. Inorg. Chem.*, 2016, 5205–5214.
13 F. Lu, PhD dissertation, Shandong University, 2014.
14 B. Anirban, C. K. Murielle, S. A. Eugen, F. Marc, J. F. Martin and A. Vincent, *Inorg. Chem.*, 2012, **51**, 7087–7093.
15 T. Zheng, H. Sun, Y. Chen, X. Li, S. Dürr, U. Radius and K. Harms, *Organometallics*, 2009, **28**, 5771–5776.
16 F. J. Weigert, *J. Org. Chem.*, 1980, **45**, 3476–3483.
17 Z. Lian, X. Xu, H. Sun, Y. Chen, T. Zheng and X. Li, *Dalton Trans.*, 2010, **39**, 9523–9529.
18 Y. Chen, H. Sun, U. Flörke and X. Li, *Organometallics*, 2008, **27**, 270–275.
19 (*a*) F. Lu, H. Sun, L. Wang and X. Li, *Inorg. Chem. Commun.*, 2014, **43**, 110–113; (*b*) F. Lu, H. Sun and X. Li, *Chin. J. Chem.*, 2013, **31**, 927–932.
20 Q. Niu, H. Sun, X. Li, H.-F. Klein and U. Flörke, *Organometallics*, 2013, **32**, 5235–5238.
21 H. Zhou, H. Sun, S. Zhang and X. Li, *Organometallics*, 2015, **34**, 1479–1486.
22 H.-F. Klein and H. H. Karsch, *Chem. Ber.*, 1975, **108**, 944–955.